1 **Archive of bacterial community in anhydrite crystals from a**

2 **deep-sea basin provides evidence of past oil-spilling in a**

3 **benthic environment in the Red Sea**

6 Yong Wang[1,2], Tie Gang Li[3,4], Meng Ying Wang[1], Qi Liang Lai[5], Jiang Tao Li[6], Zhao

7 Ming Gao[1], Zong Ze Shao[5], Pei-Yuan Qian[2,*]

8 [1]Institute of Deep-Sea Science and Engineering, Chinese Academy of Sciences, San Ya,

9 China

10 [2] Division of Life Science, Hong Kong University of Science and Technology, Clear

11 Water Bay, Hong Kong, China

12 [3] Key Laboratory of Marine Sedimentology and Environmental Geology, First Institute of

13 Oceanography, State of Oceanic Administration (SOA), Qingdao, China

14 [4]Laboratory for Marine Geology, Qingdao National Laboratory for Marine Science and

15 Technology, Qingdao, China

16 [5] Key Laboratory of Marine Biogenetic Resources, The Third Institute of Oceanography,

17 SOA, Xiamen, China

18 [6] State Key Laboratory of Marine Geology, Tongji University, Shanghai, China

19 **Corresponding author:** boqianpy@ust.hk, Tel: 852-2358-7331

20 **Keywords:** *Alcanivorax*; metagenome; anhydrite; Atlantis II brine pool; hydrothermal

21 sediment

23 **Running title:** Archive of microbial inhabitants in anhydrites

25 **Abstract**

26 In deep-sea sediment, the microbes present in anhydrite crystals are potential markers of

27 the past environment. In the Atlantis II Deep, anhydrite veins were produced by mild

28 mixture of calcium-rich hydrothermal solutions and sulfate in the bottom water, which

29 had probably preserved microbial inhabitants in the past seafloor of the Red Sea. In this

30 study, this hypothesis was tested by analyzing the metagenome of an anhydrite crystal

31 sample from the Atlantis II Deep. The estimated age of the anhydrite layer was between

32 750-770 years, which might span the event of hydrothermal eruption into the benthic

33 floor. The 16S/18S rRNA genes in the metagenome were assigned to Bacteria, Archaea,

34 Fungi and even invertebrate species. The dominant species in the crystals was an

35 oil-degrading *Alcanivorax borkumensis* bacterium, which was not detected in the adjacent

36 sediment layer. Fluorescence microscopy using 16S rRNA and marker gene probes

37 revealed intact cells of the *Alcanivorax* bacterium in the crystals. A draft genome of *A.*

38 *borkumensis* was binned from the metagenome. It contained all functional genes for

39 alkane utilization and the reduction of nitrogen oxides. Moreover, the metagenomes of

40 the anhydrites and control sediment contained aromatic degradation pathways, which

41 were mostly derived from *Ochrobactrum* sp. Altogether, these results indicate an oxic,

42 oil-spilling benthic environment in the Atlantis II basin of the Red Sea in approximately

43 the 14th century. The original microbial inhabitants probably underwent a dramatic

44 selection process via drastic environmental changes following the formation of an

45 overlying anoxic brine pool in the basin due to hydrothermal activities.

46

47

48

1. Introduction

Deep-sea sediment is among the least explored biospheres on Earth. Indigenous microbes differ vastly in community composition and metabolic spectra at different depths and sites (Orcutt et al., 2011;Teske and Sorensen, 2007). The distribution of microbes in subsuperficial sediments is determined by the porosity, nutrient availability and geochemical conditions of the sediment (Parkes et al., 2000;Webster et al., 2006). In return, genomic features and the community composition of the indigenous microbial inhabitants may reflect the *in situ* conditions and serve as biomarkers containing the geochemical indicators. However, most of the biomarkers cannot be well preserved and will be degraded by biological and abiological activities. Although lipids and other organic carbons present in some minerals allow the interpretation of microbial activities to some extent (Brocks et al., 2005), the original metabolic activities are difficult to retrieve in a comprehensive and precise manner.

Most of the dead microbes are damaged during the sedimentation process, but some can be maintained in almost their original shape (Taher, 2014;Benison et al., 2008). Evaporites, which mostly consist of halite and anhydrite ($CaSO_4$) or gypsum ($CaSO_4 \cdot 2H_2O$, temperature <38℃ (Hill, 1937)), are common microbialites with accretionary organosedimentary structures (Dupraz et al., 2011). Numerous dead bacteria, algae and metazoans have been detected in gypsum granules (Petrash et al., 2012;Trichet et al., 2001); bacterial mats growing on evaporites may become trapped and constitute much larger microbialites (Babel, 2004). Consequently, microbial inhabitants on the benthic surface may get trapped in the evaporites (Benison et al., 2008). Anhydrite facies are not found throughout deep-sea sediments. They usually form around hydrothermal vents in deep-sea environments (Jannasch and Mottl, 1985). A strong deep-sea volcanic eruption may break the crustal basalts, resulting in a drastic emission of hydrothermal gases followed by the crystallization of anhydrites and the deposition of metal sulfides (Kristall et al., 2006). An alternative model is that mild hydrothermal activities lead to a slow influx of solutions into the overlying sediment at temperatures in the sub-seafloor ranging from 20-100℃. This process also results in the formation of crystalline anhydrites in veins and around warm vents (Jannasch and Mottl, 1985). The latter process

80   may trap microbial inhabitants on the seafloor and within surface layers in anhydrites.

81   Due to the mild temperature, the trapped bodies are better preserved as excellent

82   biological evidence for past geochemical conditions.

83

84   A similar mild hydrothermal field is present in the Red Sea. Initially found in a deep-sea

85   rift in the 1960s (Swallow and Crease, 1965;Girdler, 1970), the temperature of the

86   Atlantis II brine pool has recently increased to 68°C (Anschutz and Blanc, 1996). In 1972,

87   several sediment cores were obtained from the southwest region of the pool (DSDP

88   Site226), and metal sulfides and evaporites were recognized as major mineral facies in

89   this brine-filled basin (Party, 1974). In particular, thick and well-crystalized anhydrite

90   layers were found within the hematite and at the bottom of the cores. Two major

91   anhydrite units were later defined by analysis of the adjacent core samples. The lower

92   unit comprised anhydrite ranging from 12 to 70 wt% (Anschutz et al., 2000). The

93   anhydrite in the sediments likely resulted from a geyser-type eruption of hydrothermal

94   solutions into the Atlantis II brine pool followed by the mixing of calcium-rich solutions

95   with dissolved sulfate-bearing brine and the precipitation of anhydrites during the cooling

96   process (Ramboz et al., 1988). The discovery of veins containing sulfides and anhydrite

97   in the sediment suggests that a mild hydrothermal eruption created the anhydrite facies in

98   the Atlantis II sediment (Zierenberg and Shanks, 1983;Oudin et al., 1984;Missack et al.,

99   1989). The formation of anhydrite facies in this manner would trap microbial cells and

100   organic debris in the bottom water and surface sediment. These anhydrite layers probably

101   contained important indigenous microbial inhabitants during the occurrence of the

102   hydrothermal events at the deep-sea benthic floor of the Red Sea. Coupled with [14]C

103   markers to estimate age, the anhydrite facies contained a large quantity of information

104   regarding the past geochemical changes. The formation process of the Atlantis II brine

105   pool is still controversial, largely because the source of the brine is uncertain (Schardt,

106   2016). The brine water had converted the bottom of the deep into anoxic, hypersaline and

107   hot environment. The microbes in the anhydrite facies may provide hints for the original

108   benthic conditions and age of the pool. It is also an interesting question whether oil was

109   generated in the sediments under the mild hydrothermal activities in the past deep. If yes,

110 seeping hydrothermal solutions may bring oil into the seafloor of the deep, which might

111 be documented by the microbes in the anhydrites.

112

113 In the present study, we sampled a sediment core near Site226 and detected an anhydrite

114 layer. The dominant species were alkane- and oil-degrading bacteria indicating an oxic,

115 oil-spilling benthic condition when the layer was formed. The present study sheds light

116 on the importance of anhydrites in deep-sea sediment as an archive of microbial

117 inhabitants that can serve as biomarkers of past geochemical events.

118

119 **2   Materials and methods**

120 **2.1 Physicochemical measurements of sediment layers**

121 In 2008, a 2.25-meter gravity sediment core was obtained from the southwest basin

122 (approximately 2180 meters below sea level) of the Atlantis II Deep (21°20.76' N,

123 38°04.68' E) in the Red Sea (Fig. S1) (Bower, 2009). The core was frozen at -80°C and

124 then sliced aseptically into seventy-five 3-cm sections. Microbes from sediment slices of

125 12-15 cm, 63-66 cm, 105-108 cm, 183-186 cm, and 222-225 cm were first suspended in

126 phosphate-buffered saline and shaken on a vortexer for 30 s. After 30 minutes, the

127 supernatant was filtered through a 0.22-µm black polycarbonate filter. After

128 6-diamidino-2-phenyloindole (DAPI) staining, the microbes from each layer were

129 counted under an epifluorescence microscope (n = 3) (Gough and Stahl, 2003). The pore

130 water from the above 5 layers was collected by centrifugation. The concentration of

131 dissolved organic carbon (DOC) in the pore water was determined using the combustion

132 method (Trichet et al., 2001). The concentrations of ammonium, nitrite and nitrate were

133 measured using a TNM-I analyzer (Simadzu, Kyoto, Japan). To separate large particles

134 (>63 µm) from small particles (<63 µm), the sediment samples were passed through a

135 63-µm stainless steel sieve. The percentage of small particles (dry weight) was calculated

136 for all slices.

137

138 The age of the sections was estimated with a radiometric dating method that utilizes the

139 naturally occurring radioisotope ^{14}C. The monospecific *Globigerinoides sacculifer*

140 specimens ranging in size from 250 to 350 µm were manually selected with caution and

141 then subjected to ^{14}C measurement in the National Ocean Sciences Accelerator Mass

142 Spectrometry (AMS) Facility at the Woods Hole Oceanographic Institute, USA. The raw

143 AMS ^{14}C ages were converted to calendar ages using the CALIB 6.0 program

144 (http://calib.qub.ac.uk/calib/) with the dataset Marine 09 (Reimer et al., 2009). A

145 reservoir correction has been considered for the ^{14}C difference between atmospheric and

146 surface waters (Bard, 1988).

147

148 **2.2 DNA extraction and amplification**

149 The boundary of the anhydrite layer was determined by naked eye observation and

150 particle size measurement. Crystals were manually collected from the layers, followed by

151 ultrasonic cleaning. The homogenized crystals were then analyzed by X-ray

152 diffraction (XRD) (Rigaku, Tokyo, Japan) using Cu K-alpha radiation of 40 kV and 30

153 mA. The following procedure was conducted for DNA extraction from the crystals with

154 caution to avoid contamination. Surface contamination was removed by rinsing with 70%

155 alcohol in autoclaved distilled deionized water, followed by pulsed ultrasonic cleaning

156 for 2 hours. Anhydrite crystals (20 g) (Fig. 1A) of different sizes were treated with 1 µL

157 (2U) Turbo DNase I (Ambion, Austin, Texas, US) for 30 m in a 37°C incubation before

158 being ground for DNA extraction in a sterile hood. The anhydrite powder was used for

159 DNA extraction with the PowerSoil DNA Isolation kit (MO-BIO, Carlsbad, USA),

160 followed by a purification step according to the manufacturer's instructions. Twenty

161 picograms of the raw DNA extract was used for DNA amplification using a MALBAC

162 kit (Yikang, Jiangsu, China) according to the manufacturer's manual (Zong et al., 2012).

163 The MALBAC amplification method has been evaluated recently in metagenomic studies

164 (Wang et al., 2016). Two MALBAC amplification assays were conducted using

165 twenty-one PCR cycles to acquire a sufficient amount of DNA for subsequent sequencing.

166 A negative control was also incorporated in the assay. The DNA concentration of the

167 MALBAC-amplified sample and the negative control was measured with a Bioanalyzer

168 (Agilent, CA, US). The products of the MALBAC amplification and negative control

169 were examined by gel electrophoresis to confirm the size ranges of the amplicons. Three

170 replicates of MALBAC amplifications for each sample were mixed and used for Illumina

171 sequencing on a Hiseq2500 platform (Illumina, San Diego, US). As a control, 10 g of

172 sediment from a position at 168 cm from the top of the core was used for DNA extraction.

173 There were no recognizable anhydrite crystals in this layer. DNA amplification and

174 sequencing were conducted as described above.

175

176 **2.2 Binning of metagenomes**

177 The initial Illumina 2×110-bp paired-end reads were subjected to quality assessments

178 using the NGS QC Toolkit with default parameters (Patel and Jain, 2012). The Illumina

179 sequencing data were deposited in the NCBI SRA database (accession number

180 SRA356974). The 35-bp MALBAC adapters at the start of the sequencing reads were

181 removed. Assembly of the trimmed Illumina 2×75-bp paired-end reads was performed

182 using SPAdes 3.5 (Nurk et al., 2013). The read coverage for the assembled contigs was

183 calculated using SAMtools (Li et al., 2009). The 16S/18S rRNA genes in the contigs

184 were identified using rRNA_HMM (Huang et al., 2009). Using classify.seqs command in

185 mothur package (http://www.mothur.org), taxonomic sorting of the 16S rRNA genes was

186 conducted against the SILVA database with a confidence threshold of 80%. The relative

187 abundance of the species in the metagenomes was roughly estimated based on the

188 coverage of the 16S/18S rRNA genes. Binning of the draft genomes was performed based

189 on the read coverage and G+C content of the contigs (Fig. 1B), followed by principal

190 component analysis (PCA) of the tetranucleotide frequencies (TNF) of their respective

191 contigs using a previously described pipeline (Fig. 1C) (Albertsen et al., 2013). The R

192 scripts for the binning process were obtained in

193 https://github.com/MadsAlbertsen/multi-metagenome. To evaluate the completeness of

194 the draft genome, conserved single-copy genes (CSCGs) were counted in the genome.

195 The CSCGs were identified by searching the CDSs against a database of essential

196 bacterial genes (107 essential genes) (Albertsen et al., 2013) using hmmsearch (3.0) with

197 default cutoffs for each protein family.

198

199 **2.3 Genomic analyses**

200 The coding DNA sequences (CDSs) of the draft genome were predicted using Prodigal

201 (version 2.60)(Hyatt et al., 2010). KEGG annotation of the CDSs was performed using

202 BLASTp against the KEGG database (Kanehisa et al., 2012) with a maximum e-value

cutoff of 1e-05. The KEGG pathways were reconstructed using the KEGG website (http://www.kegg.jp). CDSs were also annotated against the NCBI NR database, and MEGAN was used for taxonomic affiliation and SEED/subsystem annotation of the CDSs (Overbeek et al., 2005). The draft genome was submitted to NCBI (accession number LKAP00000000). The average nucleotide identity (ANI) was calculated using the algorithm integrated in the web service of EZGenome (Goris et al., 2007). The DNA-DNA hybridization (DDH) estimate value was calculated using the genome-to-genome distance calculator (GGDC2.0) with the alignment method of BLAST+ (Meier-Kolthoff et al., 2013;Auch et al., 2010a;Auch et al., 2010b).

2.4 Detection and phylogeny of 16S ribosomal RNA (rRNA) genes

The 16S rRNA gene sequence was identified from the draft genome sequence. The closest relatives based on 16S sequence similarity were determined using the web service of EzTaxon (Kim et al., 2012). The neighbour-joining phylogenetic tree was constructed using MEGA version 5.0 (Tamura et al., 2011) with the Kimura 2-parameter model. The phylogenetic tree was supported with bootstrap values based on 1000 replications.

2.5 Fluorescence *in situ* hybridization (FISH) of *Alcanivorax* bacteria

FISH probes for 16S rRNA gene of *Alcanivorax* bacteria were designed based on the 16S rRNA gene sequence extracted from the *Alcanivorax* draft genome. Two 16S rRNA fragments, 5'- CCTCTAATGGGCAGATTC-3' and 5'-CCCCCTCTAATGGGCAGA-3', were selected as candidate probes with Probe_Design in the ARB package (Ludwig et al., 2004). The coverage efficiency of the probes was then examined in the Silva database (Quast et al., 2013). The 6-FAM-labeled probe used to target the *alkB* gene was 5'-ATGGAGCCTAGATAATGAAGT-3' (Wang et al., 2010). A pure culture of *Alcanivorax borkumensis* Sk2 was first used to examine the probes before performing the assay, and a culture of *Escherichia coli* was used as a negative control. Two grams of anhydrite crystals were sonicated for 30 min in 1 U DNase I solution. The crystals were washed with deionized water and then ground into a powder with a beadbeater in a germ-free environment. The supernatant was mixed with 37% formaldehyde (final concentration, 1-4%). To fix the cells in PBS buffer, the sample was maintained at 4°C for

234   3-4 hr. After centrifugation at 13,000 r/min for 3 min, the supernatant was discarded. The

235   remaining microbes were soaked in 200 μL of PBS buffer, followed by addition of 200 μL

236   of ethanol (Pernthaler et al., 2002). The sample was filtered through 3-μm and 0.22-μm

237   membranes sequentially (diameter, 25 mm; Millipore, Eschborn, Germany). After

238   dehydration of the membrane using alcohol, 2 μL of dying solution containing

239   oligonucleotide probes and 20 μL of buffer (360 μL of 5 M NaCl,40 μL of 1 M Tris/HCl,

240   700 μL of 100% formamide,2 μL of 10% SDS,and water to a total volume of 2 mL).

241   The hybridization of the probes to the microbes was performed for 2 h at 46℃. Rinsing

242   buffer (700 μL of 5 M NaCl, 1 mL of 1 M Tris/ HCl, 500 μL of 0.5 M EDTA, 50 μL of

243   10% SDS and water to a total volume of 50 mL) was used to remove free probes. For

244   counterstaining, 50 μL of 4', DAPI solution (1 μg/mL) was added to the sample. After

245   incubation for 3 min, the sample was washed in Milli-Q water (MetaPhor Bioproducts,

246   Rockland, Maine) and 96% ethanol for 1 min (Pernthaler et al., 2002). The microscopic

247   observation was conducted using an Olympus BX51 (Olympus, Tokyo, Japan).

248

249   **3 Results**

250   **3.1 Physicochemical profile and cell counts**

251   A thick anhydrite layer was present at the bottom of the sediment core based on

252   naked-eye observation of the color and grain size. The anhydrite layer at depths ranging

253   from 177-198 cm consisted of coarse, agglutinated crystals, which corresponded to the

254   high percentage of large grains (78 wt% larger than 63 μm) (Fig. 2). The XRD analysis

255   further confirmed that the crystals in this layer were anhydrite. In contrast, halite

256   comprised the evaporites at depths of 12 cm, 63 cm, 105 cm and 222 cm. For the samples

257   at different depths, the DOC concentration was measured, and the highest value was

258   recorded at 183 cm (80.9 mg L^{-1}), which was even higher than the surface layer at 12 cm

259   (Fig. 3). In the 12 cm layer, the cell density was 3.2×10^5 cells per cm^3, whereas in the

260   layers at 63 cm, 105 cm and 222 cm, it was reduced by 88%, 92% and 96%, respectively

261   (Fig. 3). The cell density was also calculated as the number of cells per gram of sediment.

262   The results revealed a value of 7.1×10^5 cells per gram at a depth of 12 cm, which declined

263   more than 70% in the deeper layers. Although the cell density in the 183 cm layer

264 $(6.7 \times 10^4$ cells/cm^3) was markedly lower than that in the 12 cm layer, it was higher than

265 those in the 105 cm and 222 cm layers.

266

267 The sediment as a whole is a highly reductive environment, as indicated by the low

268 nitrate, low nitrite and extremely high ammonium concentrations (Fig. 3). To determine

269 the time of the anhydrite layers at 177-198 cm, an age estimate was performed for several

270 layers. The sediment ages were estimated based on the radioisotope ^{14}C of *G. sacculifer*

271 assuming a linear increment from the top (Fig. 2). The results obtained for the layers

272 above and below the anhydrite layer indicated a narrow range of 750-770 years between

273 153 cm and 198 cm (Table 1).

274

275 **3.2 Draft genome of the dominant bacterial species in anhydrites**

276 DNA was extracted from the anhydrite crystals and the adjacent layer separately. After

277 amplification, about 16 Gbp Illumina sequencing data were obtained and then assembled.

278 The size of the anhydrite and control metagenomes was 59 and 84 Mbp, respectively,

279 after assembly. The microbial communities differed remarkably according to the

280 taxonomic assignment of the 16S/18S rRNA gene fragments in the two metagenomes

281 (Fig. 4). At the genus level, only *Ochrobactrum* and *Alkanindiges* were common

282 inhabitants in both samples. *Alcanivorax* and *Bacillus* were also dominant genera in the

283 anhydrite and the control, respectively. At the phylum level, excluding the Proteobacteria,

284 the two metagenomes had distinctive phyla. The anhydrite contained archaea that were

285 represented by the methanogenic *Methanoculleus* (Barret et al., 2012); and fungi that

286 consisted of the Ascomycota. In contrast, the control sediment contained mainly

287 Firmicutes, Bacteroides, Actinobacteria, and Deinococcus-Thermus. At last, an

288 invertebrate species, *Prototritia* sp. belonging to Arthropoda, was identified in the

289 anhydrite.

290

291 **3.3 Genome binning of an *Alcanivorax borkumensis* genome**

292 The binned draft genome from the anhydrite metagenome was 3,069,971 bp and

293 comprised 77 contigs. A partial 16S rRNA gene sequence (805 bp) was extracted from

294 the draft genome. Because the sequence was almost identical to that of *A. borkumensis*

295   Sk2 (99.9%) (see also genomic alignment in Fig. S2), we considered the binned draft

296   genome to be from a strain of *A. borkumensis*. As shown in Figure 5, a phylogenetic tree

297   based on the 16S rRNA gene sequences of the genus *Alcanivorax* indicated that the strain

298   clustered with *A. borkumensis* Sk2, an exclusive and ubiquitous hydrocarbon-degrading

299   bacterium (Schneiker et al., 2006;Sabirova et al., 2011). The strain name of the *A.*

300   *borkumensis* in the sediment core was ABS183. It was the only microbial species that

301   could be reliably separated from the metagenome.

302

303   The genome of *A. borkumensis* ABS183, despite containing gaps, was slightly smaller

304   than that of *A. borkumensis* Sk2 (accession number NC_008260; 3,120,143 bp),

305   suggesting that the draft genome of *A. borkumensis* ABS183 was nearly complete. Also,

306   there were not detectable alignment gaps between the two genomes (Fig. S2). The

307   identification of a complete list of single-copy genes also supported the completeness of

308   the genome. The DDH estimation between *A. borkumensis* ABS183 and Sk2 was

309   97.1%±1.3%, which was higher than the standard cut-off value of 70% for genome

310   relatedness between pairs of species (Wayne et al., 1987). The ANI value between

311   ABS183 and Sk2 was 99.9%, which was also higher than the standard ANI criterion for

312   species identity (95%–96%) (Richter and Rossello-Mora, 2009). These results further

313   confirmed that ABS183 was a strain of *A. borkumensis*.

314

315   The genome of *A. borkumensis* ABS183 contains two copies of the alkane-1

316   monooxygenase gene (*alkA*; 10502_28 and 2890_35), which is an essential functional

317   gene for alkane utilization by *Alcanivorax* bacteria (Fig. 6) (Schneiker et al., 2006).

318   Neighboring the *alkA* genes, *alkBGHJ* genes, a GntR family transcriptional regulator

319   gene, and a rubredoxin gene were identified. The gene order of the related genes was

320   consistent with that of the homologs in the genome of strain Sk2 (Schneiker et al., 2006).

321   The *alk* genes were completely absent from the control metagenome. Moreover, the

322   genome of *A. borkumensis* ABS183 contains genes responsible for the reduction of

323   nitrogen oxides (KEGG genes: K00370-K00374 and K00362-K00363; nitrate reductase I

324   genes and nitrite reductase genes). The reduction process was believed to generate

325   ammonia for the efficient synthesis of amino acids (Schneiker et al., 2006). Ammonia

326   might be generated through nitrogen fixation as indicated by the presence of the related

327   genes (Fig. 6). A high demand for fatty acids was a characteristic of *A. borkumensis* to

328   perform rapid energy and organic carbon storage. *A. borkumensis* ABS183 was probably

329   able to synthesize long fatty acids because the *fas* and *fabBFGIKZ* genes responsible for

330   the elongation of fatty acids were all present in its draft genome. In contrast, the essential

331   *fas* gene (K11533) and other relevant genes were not found in the control metagenome.

332   Crude oil generally contains aromatic compounds, and the current sediment at the

333   sampling site also contained oil (Wang et al., 2011). As expected, the two metagenomes

334   possessed a complete set of genes responsible for the degradation of aromatic compounds.

335   Based on the homology of the genes, the *Ochrobactrum* and *Alkanindiges* species

336   probably played a role in this degradation.

337

338   **3.4 Detection of bacteria in anhydrite crystals by DAPI and FISH**

339   To determine whether complete microbial cells could be maintained in the anhydrite

340   crystals, DAPI and FISH assays were conducted to visualize the microbes. The DAPI

341   results revealed the presence of complete cells that were released or embedded in the

342   crystals (Fig. 7A, D, and H). However, the FISH assay, which was used to detect *A.*

343   *borkumensis* ABS183 with two probes specific to the 16S rRNA gene, showed some

344   fluorescence-labeled microbes (Fig. 7B, E and I). These microbes could also be

345   envisioned with the FISH assay using the *alkB* gene probe (Fig. 7F and 7J). The *alkB* is

346   one of the functional genes that participate in alkane degradation (Schneiker et al., 2006).

347   The rod shape of the fluorescent microbes is consistent with the microscopic features

348   reported previously (Sabirova et al., 2011). These results indicated that some microbes in

349   the microscopic fields were *A. borkumensis* ABS183, as revealed in the anhydrite

350   metagenome.

351

352   **4 Discussion**

353   In the present study, we detected complete microbial cells and analyzed their

354   metagenome in the anhydrite crystals from a deep-sea anoxic basin. The dominant

355   bacterial species was *A. borkumensis* ABS183, an aerobic bacterium that is capable of

356   degrading alkanes in crude oil. *Alcanivorax* is one of the bacterial indicators for the

357 spilling of oil in waters and surface sediment (Yakimov et al., 2007). However, the
358 Atlantis II brine pool is anaerobic and increasingly hydrothermal (Bougouffa et al.,
359 2013b). The brine sediment in the basin was also found to be anoxic. Thus, *A.*
360 *borkumensis* ABS183 could not be current inhabitants of the hydrothermal anoxic basin.
361 This difference did not explain the stratification of microbial communities in the different
362 sediment layers of the brine-filled basin. A recent study showed that *Alcanivorax* was not
363 present in all sediment layers of a sediment core from the Atlantis II basin (Wang et al.,
364 2015). A reasonable explanation for this finding is that the anhydrite layer at 177-198 cm
365 in the sediment core was formed at a previous benthic site when hydrothermal solution
366 was injected into the seafloor. The organisms living in the benthic water and subsurface
367 sediment were subsequently sealed and protected in the anhydrite crystals. Because the
368 metabolism of *A. borkumensis* bacteria was specifically used for the degradation of
369 alkanes and other hydrocarbons in crude oil (Yakimov et al., 2007), the benthic site in
370 which the anhydrite layer formed was probably an oil-spilling or oil-forming environment
371 in the Atlantis II basin. The current hot sediments in the basin are biogenic and abiogenic
372 sources of crude oil (Simoneit, 1988). Seeping of the oil has resulted in proliferation of *A.*
373 *borkumensis* bacteria in the bottom water. Similarly, oil-utilizing bacteria were nourished
374 after the oil-spilling disaster in the Gulf of Mexico (Gutierrez et al., 2013). The *A.*
375 *borkumensis* bacteria were important producers of organic carbons as they could convert
376 alkanes and nitrate into organic matter. Fatty acids and lipopolysaccharides that were
377 yielded by *A. borkumensis* bacteria were nutrients for the whole ecosystem.

378

379 Based on the results in the present study, we proposed that mild eruptions of
380 hydrothermal solutions injected calcium-rich solutions into the seafloor and produced
381 anhydrite veins by mixing with sulfate in the bottom water of the Atlantis II rift basin.
382 The anhydrite layer was then covered by sulfide minerals and biological debris such as
383 the planktonic foraminifera *G. sacculifer*. In this study, we narrowed the age of the thick
384 anhydrite layer to 750-770 years using ^{14}C isotope of the *G. sacculifer* specimens. This
385 result also indicates a relatively young sediment age and a high accumulation rate of
386 precipitated metals in the Atlantis II basin. Because the upward movement of
387 hydrothermal solutions might transfer some foraminifera specimens from lower layers to

388   the anhydrite layer, we did not use the foraminifera between anhydrite crystals. In our

389   previous study, we have shown evidence of oil formation in the Atlantis II brine pool

390   (Wang et al., 2011). The organic carbon content can be converted to aromatic compounds

391   under the hydrothermal conditions in the pool based on chemical and metagenomic

392   evidence (Wang et al., 2011). However, the bottom of the anoxic brine pool was not a

393   habitat of *Alcanivorax* species (Bougouffa et al., 2013a;Blanc and Anschutz, 1995),

394   suggesting that *Alcanivorax* flourished in the basin before the formation of brine water

395   layers over the sediment (Blanc and Anschutz, 1995).

396

397   Although there were differences in microbial communities between the anhydrite crystals

398   and the control sediment, *Ochrobactrum* sp. was one of the common inhabitants.

399   Previous studies have shown that *Ochrobactrum* species could metabolize aromatic

400   compounds aerobically and anaerobically (Zu et al., 2014;Mahmood et al., 2009), which

401   explains their presence in both metagenomes assessed in the current study. Moreover, we

402   determined the concentrations of nitrogen oxides in the different sulfide layers, although

403   only low concentrations were detected. *Ochrobactrum* species were potentially able to

404   anaerobically degrade polycyclic aromatic compounds using nitrate as an oxygen donor

405   (Mahmood et al., 2009;Wu et al., 2009). Such a chemolithoheterotrophic lifestyle is in

406   accordance with the current *in situ* environment of the sediment in the Atlantis II.

407   Regardless of the environmental changes indicated by the findings in the present study,

408   the spreading of *Ochrobactrum* sp. was seemingly not affected. Although the

409   metagenomes in the present study contained an abundant essential genes for degrading a

410   variety of aromatic compounds, the microbial degradation of these compounds might

411   have been attenuated by a lack of oxygen and a high level of salinity (Klinkhammer and

412   Lambert, 1989). Anaerobic degradation of compounds is more difficult than aerobic

413   degradation, often requiring oxygen donors such as nitrate and sulfate (Mahmood et al.,

414   2009;Wu et al., 2009). Based on its ability to survive under anoxic conditions,

415   *Ochrobactrum* sp. is probably able to maintain a higher level of fitness in the control

416   sediment compared with *Alcanivorax*. In the present study, the *Alkanindiges* identified in

417   both metagenomes was also a well-known alkane degrader (Klein et al., 2007;Bogan et

418   al., 2003). Because of its presence in both anhydrites and the adjacent sulfide layer, we

419   assumed that the *Alkanindiges* bacterium was also capable of surviving aerobically and

420   anaerobically in the oil-producing sediment. Hence, the change from an oxic to an anoxic

421   benthic environment caused a dramatic shift in the microbial communities, resulting in

422   the extinction of the obligate aerobic alkane-utilizer *Alcanivorax* and continuous

423   residency of anaerobic oil-degraders. The availability of nitrogen oxides and the

424   dissolution of sulfate from anhydrite crystals were possibly critical to the metabolic

425   activities of the anaerobes. In addition, the *Bacillus* and fungi present in the control

426   sediment were probably present in the form of dormant spores. In a recent report,

427   *Ochrobactrum* and *Bacillus* were confirmed to be dominant species in some upper sulfide

428   layers in the Atlantis II (Wang et al., 2015). Altogether, in the present study, the current

429   microbial inhabitants in the sulfide layers were largely different from those in the

430   anhydrite crystals.

431

432   The geochemical data collected herein suggested that the sub-superficial anhydrite layer

433   could release organic carbon contents into the sediment, as reported previously [12,13]. Our

434   measurement of DOC at 80.9 mg L^{-1} in the anhydrite layer was higher than the generally

435   accepted maximum value of 50 mg L^{-1} for marine sediments (Cameron et al., 2006). The

436   abnormally high DOC was considered a notable alteration of the local environments,

437   probably resulted from the breakdown of anhydrite crystals. Anhydrites in the Atlantis II

438   brine sediment were likely maintained by the high salinity and temperature, and then

439   slowly dissolved. This phenomenon may be explained by the slight undersatuation of the

440   anhydrite in the Atlantis II sediment (Anschutz et al., 2000). Such anhydrite layers are

441   widely distributed in Middle Eastern sediments (Alsharhan and Nairn, 1997). Hence, our

442   findings shed light on the formation of micro-environments by anhydrite evaporites in the

443   deep sediments. In this study, there was an inconsistency between the cell density and the

444   DOC at the 12-cm depth layer, in which the DOC could not support a 10-fold higher

445   biomass. This phenomenon probably resulted from the formation of petroleum

446   compounds under the hydrothermal effects (Wang et al., 2011). In the petroleum,

447   hydrophobic organic compounds (HOCs) consisting of polycyclic aromatic hydrocarbons

448   (PAHs) could not be counted in our DOC measurements (personal communication with J.

449   Pearsons). The nutrient supply is critical for microbes to survive in deep-sea sediment.

450 Apart from the chemolithoautotrophic microbes, numerous other inhabitants take
451 advantage of the buried organic matter. Importantly, the trapped organic matter serves as
452 a nutrient supply following the dissolution of organic-rich anhydrite crystals. Therefore,
453 our findings highlighted the importance of the nutrients released from the anhydrite facies
454 for microbes in deep-sea subsuperficial sediment.
455

456 *Author contributions.* Y. Wang, T.G. Li, and P. Y. Qian were responsible for the study
457 design. Data analysis was performed by Y. Wang, T.G. Li, J. T. Li, Q. L. Lai, and Z. M.
458 Gao. M.Y. Wang conducted FISH assay. The manuscript was prepared by Y. Wang with
459 contributions from all co-authors.
460 *Acknowledgments.* This study was supported by the National Science Foundation of
461 China No. 41476104 and No. 31460001 to Y. Wang, and the King Abdullah University
462 of Science and Technology (SA-C0040/UK-C0016) to P.Y. Qian. This work was also
463 supported by Hainan international collaborative grant No. KJHZ2015-22.

464

References

Albertsen, M., Hugenholtz, P., Skarshewski, A., Nielsen, K. L., Tyson, G. W., and Nielsen, P. H.: Genome sequences of rare, uncultured bacteria obtained by differential coverage binning of multiple metagenomes, Nat Biotechnol, 31, 533-538, Doi 10.1038/Nbt.2579, 2013.

Alsharhan, A. S., and Nairn, A. E. M.: Sedimentary basins and petroleum geology of the Middle East, Elsevier Science B.V., Amsterdam, 1997.

Anschutz, P., and Blanc, G.: Heat and salt fluxes in the Atlantis II Deep (Red Sea), Earth Planet Sci Lett, 142, 147-159, 1996.

Anschutz, P., Blanc, G., Monnin, C., and Boulègue, J.: Geochemical dynamics of the Atlantis II Deep (Red Sea): II. Composition of metalliferous sediment pore waters, Geochim Cosm Acta, 64, 3995-4006, 2000.

Auch, A. F., Klenk, H. P., and Goker, M.: Standard operating procedure for calculating genome-to-genome distances based on high-scoring segment pairs, Stand Genom Sci , 2, 142-148, 10.4056/sigs.541628, 2010a.

Auch, A. F., von Jan, M., Klenk, H. P., and Goker, M.: Digital DNA-DNA hybridization for microbial species delineation by means of genome-to-genome sequence comparison, Stand Genom Sci, 2, 117-134, 10.4056/sigs.531120, 2010b.

Babel, M.: Models for evaporite, selenite and gypsum microbialite deposition in ancient saline basins, Acta Geologica Polonica, 54, 219-249, 2004.

Bard, E.: Correction of accelerator mass spectrometry 14C ages measured in planktonic foraminifera: Paleoceanographic implications., Paleoceanography, 3, 635-645, 1988.

Barret, M., Gagnon, N., Morissette, B., Topp, E., Kalmokoff, M., Brooks, S. P. J., Matias, F., Massé, D. I., Masse, L., and Talbot, G.: Methanoculleus spp. as a biomarker of methanogenic activity in swine manure storage tanks, FEMS Microbiol Eco, 80, 427-440, 10.1111/j.1574-6941.2012.01308.x, 2012.

Benison, K. C., Jagniecki, E. A., Edwards, T. B., Mormile, M. R., and Storrie-Lombardi, M. C.: "Hairy blobs:" microbial suspects preserved in modern and ancient extremely acid lake evaporites, Astrobiology, 8, 807-821, 10.1089/ast.2006.0034, 2008.

Blanc, G., and Anschutz, P.: New stratification in the hydrothermal brine system of the Atlantis II Deep, Red Sea, Geology, 23, 543-546, 1995.

Bogan, B. W., Sullivan, W. R., Kayser, K. J., Derr, K. D., Aldrich, H. C., and Paterek, J. R.: Alkanindiges illinoisensis gen. nov., sp. nov., an obligately hydrocarbonoclastic, aerobic squalane-degrading bacterium isolated from oilfield soils, Int J Syst Evol Microbiol, 53, 1389-1395, 10.1099/ijs.0.02568-0, 2003.

Bougouffa, S., Yang, J. K., Lee, O. O., Wang, Y., Batang, Z., Al-Suwailem, A., and Qian, P. Y.: Distinctive microbial community structure in highly stratified deep-sea brine water columns, Appl Environ Microbiol, 79, 3425-3437, 10.1128/aem.00254-13, 2013a.

Bougouffa, S., Yang, J. K., Lee, O. O., Wang, Y., Batang, Z., Al-Suwailem, A., and Qiana, P. Y.: Distinctive microbial community structure in highly stratified deep-sea brine water columns, Appl Environ Microb, 79, 3425-3437, Doi 10.1128/Aem.00254-13, 2013b.

Bower, A. S.: R/V Oceanus Voyage 449-6 Red Sea Atlantis II Deep Complex Area 19 October-1 November 2008, Woods Hole Oceanographic Institution, 2009.

510 Brocks, J. J., Love, G. D., Summons, R. E., Knoll, A. H., Logan, G. A., and Bowden, S.
511   A.: Biomarker evidence for green and purple sulphur bacteria in a stratified
512   Palaeoproterozoic sea, Nature, 437, 866-870, 2005.
513 Cameron, D., Willett, M., and Hammer, L.: Distribution of organic carbon in the
514   Berkeley Pit lake, Butte, Montana, Mine Water Environ, 25, 93-99,
515   10.1007/s10230-006-0116-4, 2006.
516 Dupraz, C., Reid, R. P., and Visscher, P. T.: Microbialites, modern, in: Encyclopaedia of
517   Geobiology, edited by: Reitner, V., and Thiel, J., Springer, Heidelberg, 617-635, 2011.
518 Girdler, R. W.: A review of Red Sea heat flow, Phil Trans Roy Soc Lon A, 267, 191-203,
519   1970.
520 Goris, J., Konstantinidis, K. T., Klappenbach, J. A., Coenye, T., Vandamme, P., and
521   Tiedje, J. M.: DNA–DNA hybridization values and their relationship to whole-genome
522   sequence similarities, Int J Syst Evol Microbiol, 57, 81-91, 2007.
523 Gough, H. L., and Stahl, D. A.: Optimization of direct cell counting in sediment. , J
524   Microbiol Methods, 52, 39-46, 2003.
525 Gutierrez, T., Singleton, D. R., Berry, D., Yang, T., Aitken, M. D., and Teske, A.:
526   Hydrocarbon-degrading bacteria enriched by the Deepwater Horizon oil spill
527   identified by cultivation and DNA-SIP, ISME J, 7, 2091-2104, 10.1038/ismej.2013.98,
528   2013.
529 Hill, A. E.: The transition temperature of gypsum to anhydrite, J Am Chem Soc, 59,
530   2242-2244, 10.1021/ja01290a039, 1937.
531 Huang, Y., Gilna, P., and Li, W.: Identification of ribosomal RNA genes in metagenomic
532   fragments, Bioinformatics, 25, 1338-1340, 2009.
533 Hyatt, D., Chen, G. L., LoCascio, P. F., Land, M. L., Larimer, F. W., and Hauser, L. J.:
534   Prodigal: prokaryotic gene recognition and translation initiation site identification,
535   Bmc Bioinformatics, 11, Artn 119
536 Doi 10.1186/1471-2105-11-119, 2010.
537 Jannasch, H. W., and Mottl, M. J.: Geomicrobiology of deep-sea hydrothermal vents,
538   Science, 229, 717-725, 10.1126/science.229.4715.717, 1985.
539 Kanehisa, M., Goto, S., Sato, Y., Furumichi, M., and Tanabe, M.: KEGG for integration
540   and interpretation of large-scale molecular data sets, Nucleic Acids Res, 40, D109-114,
541   10.1093/nar/gkr988
542 gkr988 [pii], 2012.
543 Kim, O. S., Cho, Y. J., Lee, K., Yoon, S. H., Kim, M., Na, H., Park, S. C., Jeon, Y. S.,
544   Lee, J. H., Yi, H., Won, S., and Chun, J.: Introducing EzTaxon-e: a prokaryotic 16S
545   rRNA gene sequence database with phylotypes that represent uncultured species, Int J
546   Syst Evol Microbiol, 62, 716-721, 10.1099/ijs.0.038075-0, 2012.
547 Klein, A. N., Frigon, D., and Raskin, L.: Populations related to Alkanindiges, a novel
548   genus containing obligate alkane degraders, are implicated in biological foaming in
549   activated sludge systems, Environ Microbiol, 9, 1898-1912,
550   10.1111/j.1462-2920.2007.01307.x, 2007.
551 Klinkhammer, G. P., and Lambert, C. E.: Preservation of organic matter during salinity
552   excursions, Nature, 339, 271-274, 1989.
553 Kristall, B., Kelley, D. S., Hannington, M. D., and Delaney, J. R.: Growth history of a
554   diffusely venting sulfide structure from the Juan de Fuca Ridge: A petrological and

555   geochemical study, Geochem. Geophys. Geosyst., 7, Q07001, 10.1029/2005gc001166,
556   2006.

557 Li, H., Handsaker, B., Wysoker, A., Fennell, T., Ruan, J., Homer, N., Marth, G., Abecasis,
558   G., and Durbin, R.: The sequence alignment/map format and SAMtools,
559   Bioinformatics, 25, 2078-2079, DOI 10.1093/bioinformatics/btp352, 2009.

560 Ludwig, W., Strunk, O., Westram, R., Richter, L., Meier, H., Yadhukumar, Buchner, A.,
561   Lai, T., Steppi, S., Jobb, G., Forster, W., Brettske, I., Gerber, S., Ginhart, A. W., Gross,
562   O., Grumann, S., Hermann, S., Jost, R., Konig, A., Liss, T., Lussmann, R., May, M.,
563   Nonhoff, B., Reichel, B., Strehlow, R., Stamatakis, A., Stuckmann, N., Vilbig, A.,
564   Lenke, M., Ludwig, T., Bode, A., and Schleifer, K.-H.: ARB: a software environment
565   for sequence data, Nucl. Acids Res., 32, 1363-1371, 10.1093/nar/gkh293, 2004.

566 Mahmood, Q., Hu, B., Cai, J., Zheng, P., Azim, M. R., Jilani, G., and Islam, E.: Isolation
567   of Ochrobactrum sp.QZ2 from sulfide and nitrite treatment system, J Hazardous
568   Materials, 165, 558-565, http://dx.doi.org/10.1016/j.jhazmat.2008.10.021, 2009.

569 Meier-Kolthoff, J. P., Auch, A. F., Klenk, H. P., and Goker, M.: Genome sequence-based
570   species delimitation with confidence intervals and improved distance functions, BMC
571   Bioinfo, 14, 60, 10.1186/1471-2105-14-60, 2013.

572 Missack, E., Stoffers, P., and El Goresy, A.: Mineralogy, paragenesis, and phases
573   relations of copper iron sulfides in the Atlantis II Deep, Red Sea, Min. Deposita, 24,
574   82-91, 1989.

575 Nurk, S., Bankevich, A., Antipov, D., Gurevich, A. A., Korobeynikov, A., Lapidus, A.,
576   Prjibelski, A. D., Pyshkin, A., Sirotkin, A., Sirotkin, Y., Stepanauskas, R., Clingenpeel,
577   S. R., Woyke, T., McLean, J. S., Lasken, R., Tesler, G., Alekseyev, M. A., and
578   Pevzner, P. A.: Assembling single-cell genomes and mini-metagenomes from chimeric
579   MDA products, J Comput Biol, 20, 714-737, 10.1089/cmb.2013.0084, 2013.

580 Orcutt, B. N., Sylvan, J. B., Knab, N. J., and Edwards, K. J.: Microbial ecology of the
581   dark ocean above, at, and below the seafloor, Microbiol Mol Biol Rev, 75, 361-422,
582   Doi 10.1128/Mmbr.00039-10, 2011.

583 Oudin, E., Thisse, Y., and Ramboz, C.: Fluid inclusion and mineralogical evidence for
584   high temperature saline hydrothermal circulation in the Red Sea metalliferous
585   sediments: preliminary results, Mar. Mining, 5, 3-31, 1984.

586 Overbeek, R., Begley, T., Butler, R. M., Choudhuri, J. V., Chuang, H. Y., Cohoon, M., de
587   Crecy-Lagard, V., Diaz, N., Disz, T., Edwards, R., Fonstein, M., Frank, E. D., Gerdes,
588   S., Glass, E. M., Goesmann, A., Hanson, A., Iwata-Reuyl, D., Jensen, R., Jamshidi, N.,
589   Krause, L., Kubal, M., Larsen, N., Linke, B., McHardy, A. C., Meyer, F., Neuweger,
590   H., Olsen, G., Olson, R., Osterman, A., Portnoy, V., Pusch, G. D., Rodionov, D. A.,
591   Ruckert, C., Steiner, J., Stevens, R., Thiele, I., Vassieva, O., Ye, Y., Zagnitko, O., and
592   Vonstein, V.: The subsystems approach to genome annotation and its use in the project
593   to annotate 1000 genomes, Nucl Acids Res, 33, 5691-5702, 33/17/5691 [pii]
594 10.1093/nar/gki866, 2005.

595 Parkes, R. J., Cragg, B. A., and Wellsbury, P.: Recent studies on bacterial populations
596   and processes in subseafloor sediments: A review, Hydrogeol J, 8, 11-28,
597   10.1007/pl00010971, 2000.

598 Party, T. S. S.: Red Sea: Site 226, in: Deep Sea Drilling Project, 595-600, 1974.

Pernthaler, A., Pernthaler, J., and Amann, R.: Fluorescence in situ hybridization and catalyzed reporter deposition for the identification of marine bacteria, Appl Environ Microb, 68, 3094-3101, 2002.

Petrash, D. A., Gingras, M. K., Lalonde, S. V., Orange, F., Pecoits, E., and Konhauser, K. O.: Dynamic controls on accretion and lithification of modern gypsum-dominated thrombolites, Los Roques, Venezuela, Sedi Geol, 245-246, 29-47, 2012.

Quast, C., Pruesse, E., Yilmaz, P., Gerken, J., Schweer, T., Yarza, P., Peplies, J., and Glöckner, F. O.: The SILVA ribosomal RNA gene database project: improved data processing and web-based tools, Nucl Acids Res, 41, D590-D596, 10.1093/nar/gks1219, 2013.

Ramboz, C., Oudin, E., and Thisse, Y.: Geyser-type discharge in Atlantis II Deep, Red Sea: evidence of boiling from fluid inclusions in epigenetic anhydrite, Can Mineral, 26, 765-786, 1988.

Reimer, P. J., Baillie, M. G. L., Bard, E., Bayliss, A., Beck, J. W., Blackwell, P. G., Ramsey, C. B., Buck, C. E., Burr, G. S., Edwards, R. L., Friedrich, M., Grootes, P. M., Guilderson, T. P., Hajdas, I., Heaton, T. J., Hogg, A. G., Hughen, K. A., Kaiser, K. F., Kromer, B., McCormac, F. G., Manning, S. W., Reimer, R. W., Richards, D. A., Southon, J. R., Talamo, S., Turney, C. S. M., van der Plicht, J., and Weyhenmeyer, C. E.: IntCal09 and Marine09 radiocarbon age calibration curves, 0-50,000yeats cal BP, Radiocarbon, 51, 1111-1150, 2009.

Richter, M., and Rossello-Mora, R.: Shifting the genomic gold standard for the prokaryotic species definition, Proc Natl Acad Sci U S A, 106, 19126-19131, 10.1073/pnas.0906412106, 2009.

Sabirova, J. S., Becker, A., Lunsdorf, H., Nicaud, J. M., Timmis, K. N., and Golyshin, P. N.: Transcriptional profiling of the marine oil-degrading bacterium Alcanivorax borkumensis during growth on n-alkanes, FEMS Microbiol Lett, 319, 160-168, 10.1111/j.1574-6968.2011.02279.x, 2011.

Schardt, C.: Hydrothermal fluid migration and brine pool formation in the Red Sea: the Atlantis II Deep, Mineralium Deposita, 51, 89-111, 10.1007/s00126-015-0583-2, 2016.

Schneiker, S., Martins dos Santos, V. A., Bartels, D., Bekel, T., Brecht, M., Buhrmester, J., Chernikova, T. N., Denaro, R., Ferrer, M., Gertler, C., Goesmann, A., Golyshina, O. V., Kaminski, F., Khachane, A. N., Lang, S., Linke, B., McHardy, A. C., Meyer, F., Nechitaylo, T., Puhler, A., Regenhardt, D., Rupp, O., Sabirova, J. S., Selbitschka, W., Yakimov, M. M., Timmis, K. N., Vorholter, F. J., Weidner, S., Kaiser, O., and Golyshin, P. N.: Genome sequence of the ubiquitous hydrocarbon-degrading marine bacterium Alcanivorax borkumensis, Nature Biotech, 24, 997-1004, 10.1038/nbt1232, 2006.

Simoneit, B. R. T.: Petroleum generation submarine hydrothermal systems: An update, Can Mineral, 26, 827-840, 1988.

Swallow, J. C., and Crease, J.: Hot salty water at the bottom of the Red Sea, Nature, 205, 165-166, 1965.

Taher, A. G.: Microbially induced sedimentary structures in evaporite–siliciclastic sediments of Ras Gemsa sabkha, Red Sea Coast, Egypt, J Adv Res, 5, 577-586, http://dx.doi.org/10.1016/j.jare.2013.07.009, 2014.

644 Tamura, K., Peterson, D., Peterson, N., Stecher, G., Nei, M., and Kumar, S.: MEGA5:
645   molecular evolutionary genetics analysis using maximum likelihood, evolutionary
646   distance, and maximum parsimony methods, Mol Biol Evol, 28, 2731-2739, 2011.
647 Teske, A., and Sorensen, K. B.: Uncultured archaea in deep marine subsurface sediments:
648   have we caught them all?, ISME J, 2, 3-18, 2007.
649 Trichet, J., Défarge, C., Tribble, J., Tribble, G. W., and Sansone, F. J.: Christmas Island
650   lagoonal lakes, models for the deposition of carbonate-evaporite-organic laminated
651   sediments, Sedimentary Geol, 140, 177-189, 2001.
652 Wang, W., Wang, L., and Shao, Z.: Diversity and abundance of oil-degrading bacteria
653   and alkane hydroxylase (alkB) genes in the subtropical seawater of Xiamen Island,
654   Microb Ecol, 60, 429-439, 10.1007/s00248-010-9724-4, 2010.
655 Wang, Y., Yang, J., Lee, O. O., Dash, S., Lau, S. C. K., Al-Suwailem, A., Wong, T. Y. H.,
656   Danchin, A., and Qian, P.-Y.: Hydrothermally generated aromatic compounds are
657   consumed by bacteria colonizing in Atlantis II Deep of the Red Sea, ISME J, 5, 1652–
658   1659, 2011.
659 Wang, Y., Li, J. T., He, L. S., Yang, B., Gao, Z. M., Cao, H. L., Batang, Z., Al-Suwailem,
660   A., and Qian, P. Y.: Zonation of microbial communities by a hydrothermal mound in
661   the Atlantis II Deep (the Red Sea), PLoS ONE, 10, e0140766,
662   10.1371/journal.pone.0140766, 2015.
663 Wang, Y., Gao, Z. M., Xu, Y., Li, G. Y., He, L. S., and Qian, P. Y.: An evaluation of
664   multiple annealing and looping based genome amplification using a synthetic bacterial
665   community, ACTA Oceanol Sin, 35, 131-136, 2016.
666 Wayne, L. G., Brenner, D. J., Colwell, R. R., Grimont, P. A. D., Kandler, O., Krichevsky,
667   M. I., Moore, L. H., Moore, W. E. C., Murray, R. G. E., Stackebrandt, E., Starr, M. P.,
668   and Trüper, H. G.: Report of the ad hoc committee on reconciliation of approaches to
669   bacterial systematics, Int J Syst Bacteriol, 37, 463-464, 1987.
670 Webster, G., John Parkes, R., Cragg, B. A., Newberry, C. J., Weightman, A. J., and Fry, J.
671   C.: Prokaryotic community composition and biogeochemical processes in deep
672   subseafloor sediments from the Peru Margin, FEMS Microbiol Ecol, 58, 65-85,
673   10.1111/j.1574-6941.2006.00147.x, 2006.
674 Wu, Y., He, T., Zhong, M., Zhang, Y., Li, E., Huang, T., and Hu, Z.: Isolation of marine
675   benzo[a]pyrene-degrading Ochrobactrum sp. BAP5 and proteins characterization, J
676   Environ Sci, 21, 1446-1451, 2009.
677 Yakimov, M. M., Timmis, K. N., and Golyshin, P. N.: Obligate oil-degrading marine
678   bacteria, Curr Opin Biotech, 18, 257-266, 2007.
679 Zierenberg, R. A., and Shanks, W. C.: Mineralogy and geochemistry of epigenetic
680   features in metalliferous sediment, Atlantis II Deep, Red Sea, Econ Geol, 78, 57-72,
681   10.2113/gsecongeo.78.1.57, 1983.
682 Zong, C., Lu, S., Chapman, A. R., and Xie, X. S.: Genome-wide detection of
683   single-nucleotide and copy-number variations of a single human cell, Science, 338,
684   1622-1626, 10.1126/science.1229164, 2012.
685 Zu, L., Xiong, J., Li, G., Fang, Y., and An, T.: Concurrent degradation of
686   tetrabromobisphenol A by Ochrobactrum sp. T under aerobic condition and estrogenic
687   transition during these processes, Ecot Eviron Safety, 104, 220-225,
688   10.1016/j.ecoenv.2014.03.015, 2014.
689

690   **Data Accessibility**

691   Illumina raw data will be accessible under SRA356974 in the NCBI SRA database. *B.*

692   *borkumensis* ABS183 genome was deposited in the NCBI under BioProject

693   LKAP00000000 and will be public on October 31, 2016.

694

695

696   **Table 1.** Age estimates of the sediment layers

Layer (cm)	Age (year)	Age error (year)
3-6	320	25
21-24	475	35
45-48	490	30
90-93	500	25
129-132	560	35
153-156	750	30
198-201	770	30
222-225	880	30

697

698   Eight sediment layers were selected for the age estimates using radioisotope ^{14}C of *G.*

699   *sacculifer* collected from the respective layers. The age was corrected by the 400-year

700   reservoir age with an error range.

701

702

703 **Figures**

704 **Figure 1. Anhydrite crystals and genome binning.**

705 Anhydrite crystals in a Petri dish (90 mm in diameter) (A) were used for DNA extraction.

706 The amplified genomic DNA was sequenced and then reassembled. Based on the G+C

707 content and read coverage, the binned contigs with high coverage levels (B) were

708 selected for examination of the tetranucleotide frequency consistency in the PCA analysis

709 (C).

710

711
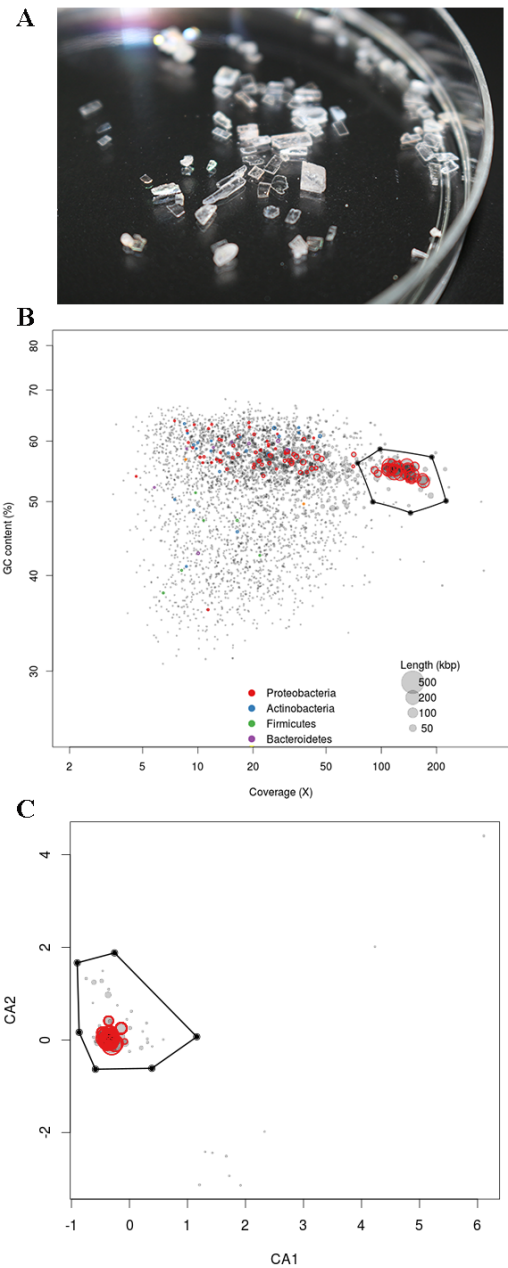
Figure 2. Grain size and age of selected layers

The percentages of the small particles (<63μm) in dry weight are shown for 75 slices of the sediment core (small squares on the line). The age estimates (black circles) of the selected layers were performed using radioisotope 14C of the monospecific *Globigerinoides sacculifer* specimens. Age errors ranged between 25 to 40 years. Anhydrite and control layers for metagenomic study were indicated by arrows.

718

719

720
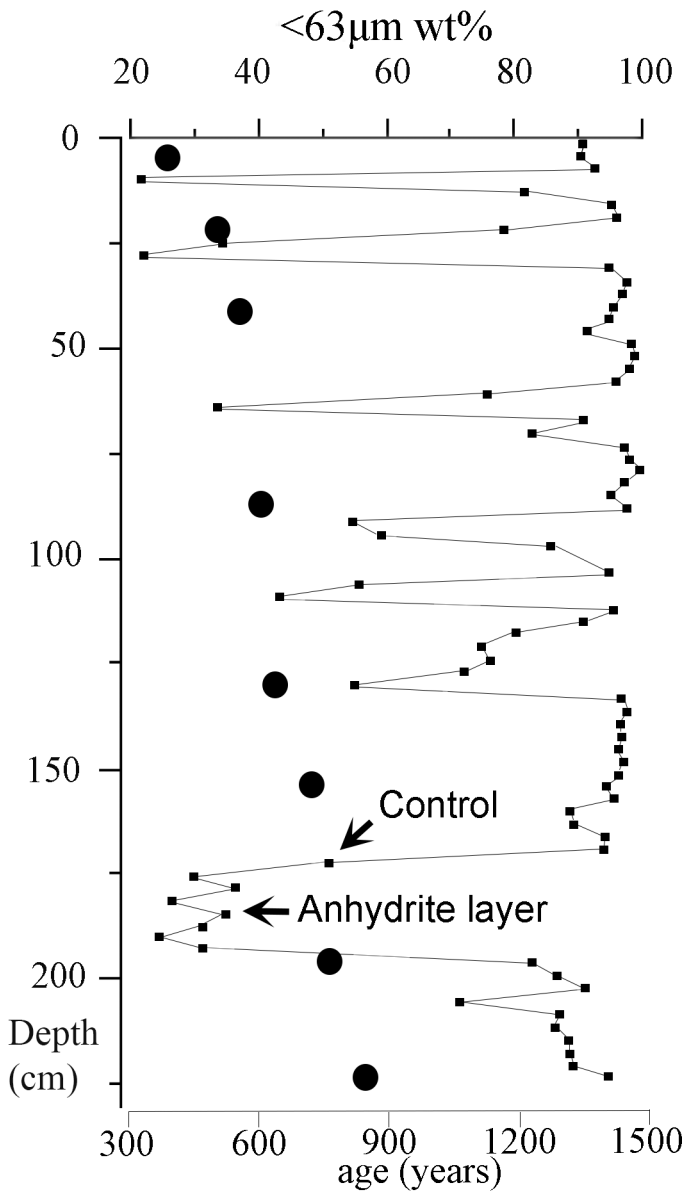
721 **Figure 3. Nutrient measurements and cell counts in the different sediment layers.**

722 The pore water samples were analyzed for five layers of a sediment core obtained from

723 the Atlantis II Deep (21°20.76' N, 38°04.68' E) in 2008. DOC: dissolved organic carbon.

724

725

726

727

728

729

730

731

732

733

734

735

736

737

738

739

740

741
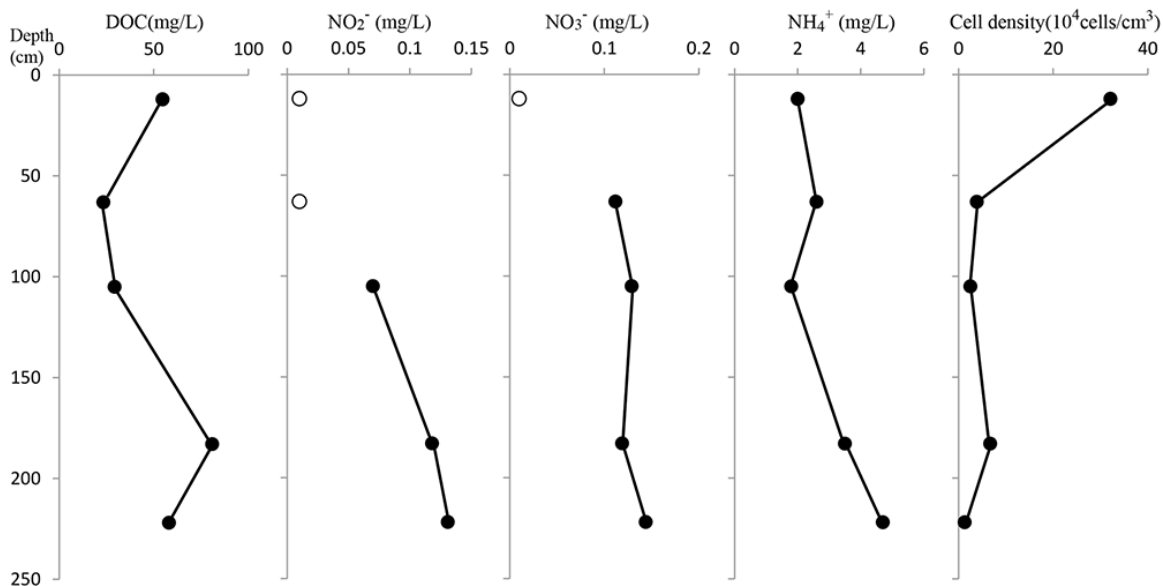
742 **Figure 4. Microbial communities in anhydrite crystals and neighboring control**

743 **sediment.**

744 Phyla and genera in the anhydrite crystals and control layer were predicted using 16S/18S

745 rRNA gene fragments extracted from the corresponding metagenomes (D-T:

746 Deinococcus-Thermus). The relative abundance of the genera can be estimated by the

747 coverage level of the 16S/18S rRNA fragments by reads.

748

749

750

751

752

753

754

755

756
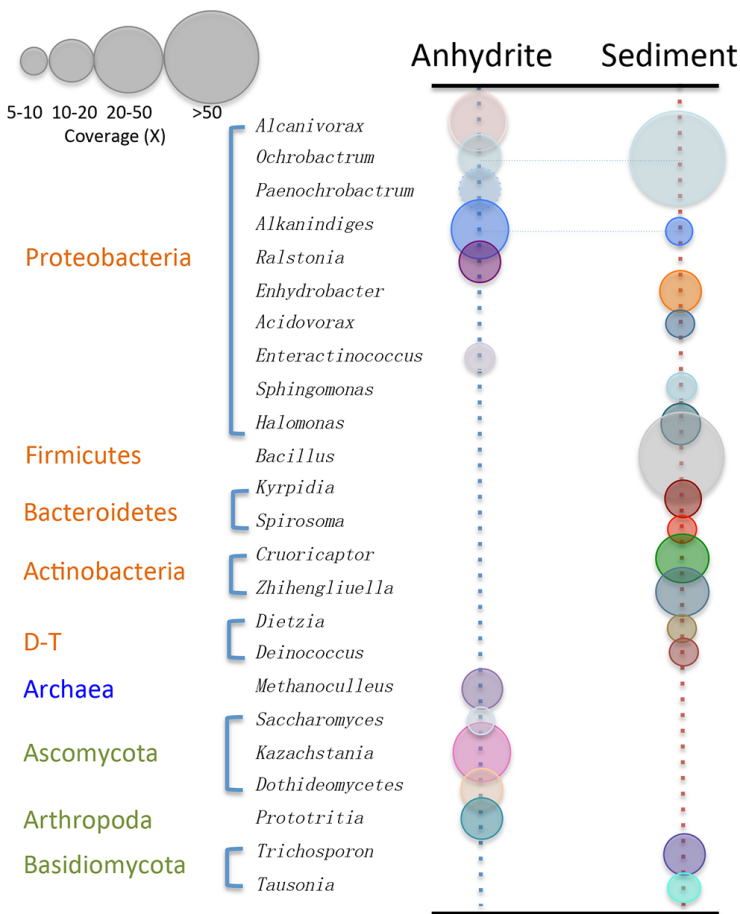
757 **Figure 5. Phylogenetic tree of 16S rRNA genes.**

758 Bootstrap values (expressed as percentages of 1000 replications) are shown at the

759 branches of the neighbor-joining tree.

760

761
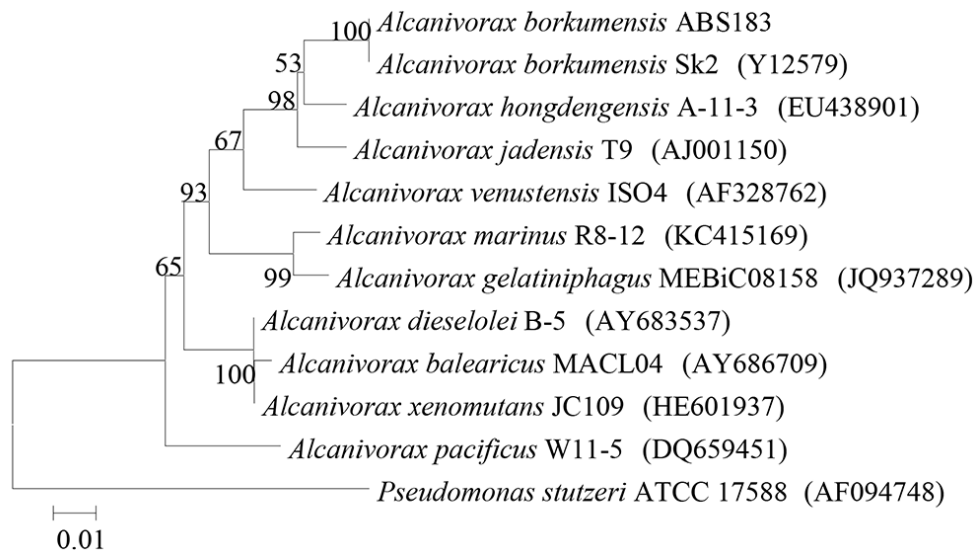
762 **Figure 6. Schematic model of metabolism and cross-membrane transporters**

763 The model was predicted based on the genes in the draft genome of *Alcanivorax*

764 *borkumensis* ABS183.

765

766

767

768
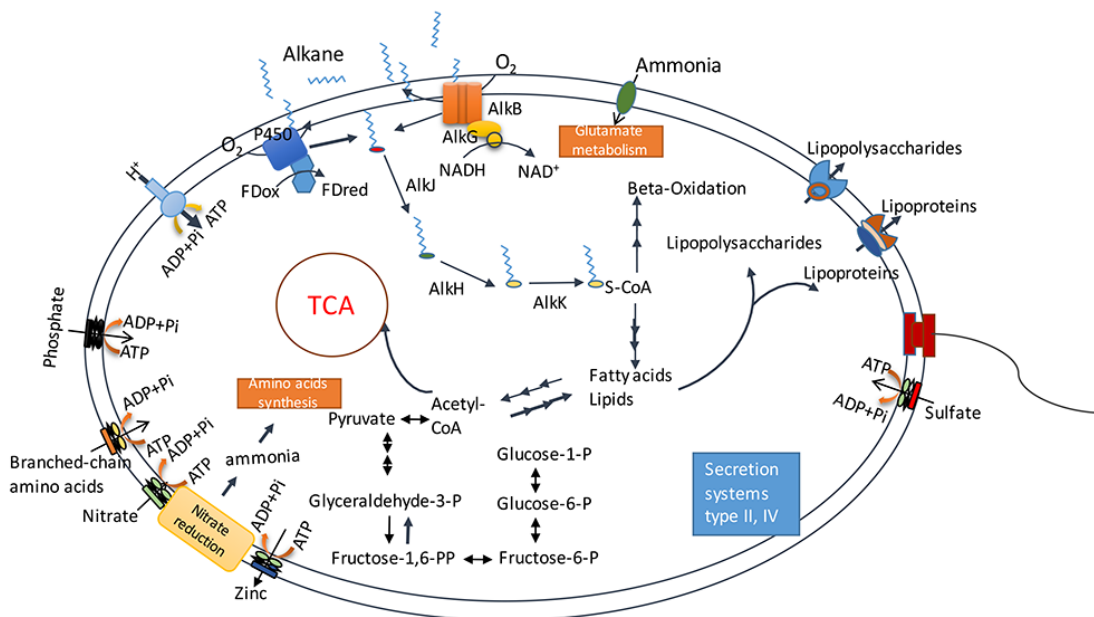
Figure 7. Fluorescence *in situ* hybridization (FISH) of *Alcanivorax* sp. ABS183 embedded in anhydrite crystals.

DAPI staining and FISH using 16S rRNA probes are shown in A and B. The merged image of A and B is shown in Fig. 7C. DAPI staining and FISH were also performed using two samples that were filtered with 3-μm (D-G) and 0.22-μm (H-K) membranes, respectively. *Alcanivorax* bacteria were released from the large crystals filtered through the 3-μm membranes (D-G). The bacteria were stained with DAPI (D), 16S rRNA probes (E) and the *alkB* probe (F), respectively, and overlaid (G). Using a sample filtered through a 0.22-μm membrane, a dividing *Alcanivorax* sp. ABS183 cell was labeled using the same method and probes (H-J). The microscopic fields shown in H-J are merged in Fig. 7K.

779

780

781